EXPERIMENTAL STUDY ON MICROBUBBLES AND THEIR APPLICABILITY TO SHIPS FOR SKIN FRICTION REDUCTION

Yoshiaki Kodama, Akira Kakugawa,
Takahito Takahashi, and Hideki Kawashima
Ship Research Institute
6-38-1, Shinkawa, Mitaka
Tokyo 181-0004, Japan

ABSTRACT

Microbubble experiments were carried out using a circulating water tunnel specially designed for testing microbubbles. Skin friction was measured using a skin friction sensor, and skin friction reduction by microbubbles up to 40% was obtained. The local void ratio in the bubble condition was measured by putting a suction tube in the test section, and it was found that the local void ratio close to the wall has strong correlation with skin friction reduction. The applicability of microbubbles to full scale ships was discussed, based on experimental results using a long flat plate.

INTRODUCTION

Tankers and bulk carriers that carry heavy loads such as crude oil, ore and grain, play an important role in the world trade. Their characteristics are that they are very large and that they move very slowly. With such ships the wavemaking drag component, which increases drastically as the speed increases, is very small, and the skin friction drag component occupies approximately 80% of the total drag, and therefore its reduction has practical importance.

Skin friction reduction of ships has its own difficulties. One is that the Reynolds number is very high. Table 1 shows the dimensions of a 150,000 tonnage tanker. The table also shows the height h of riblets, a typical skin friction reduction device, in full scale and model scale ships. The height of the riblets is estimated as follows; If one uses the local skin friction formula (Schlichting, 1968)

$$C_f' \equiv \frac{\tau_w}{\frac{1}{2}\rho U^2} = (2\log_{10}R_x - 0.65)^{-2.3} \qquad (1)$$

where R_x is the Reynolds number based on the distance from the leading edge, then the height of riblets h is expressed as

$$\frac{h}{L} = h^+ \frac{\sqrt{2}}{R_e}(2\log_{10}R_x - 0.65)^{1.15}, \qquad (2)$$

and the height of riblets h in the table is derived. It is seen that skin friction devices which are scaled with friction velocity, such as riblets, become more difficult to apply as the size of a body becomes larger. It should also be mentioned that there is a fouling problem in the sea environment, which makes the situation still more difficult.

Table 1 Estimated riblet heights for a 150,000 tonnage tanker (Froude number $F_n \equiv \frac{U}{\sqrt{gL}} \equiv 0.134$, $h^+ \equiv 15$)

Dimensions	Full scale ship	Model scale ship
Length L (m)	320	7
Breadth B (m)	60	1.31
Depth d (m)	22	0.48
Speed U (m/s)	7.5	1.11
$R_e(\equiv UL/\nu)$	2.4×10^9	7.8×10^6
h/L	2.38×10^{-7}	5.0×10^{-5}
h (mm)	0.08	0.35

Microbubbles, i.e. small bubbles injected into the boundary layer on a solid wall, reduce skin friction significantly (Merkle, 1990). They are suited to full scale ships because; (1)their experimental results are scaled with the boundary layer thickness and free-stream speed and therefore do not have the scaling problem mentioned above, (2)they are perhaps insensitive to fouling, except for air injection holes, and (3)practical hull forms of ships have a wide flat bottom, along which the bubbles injected in the front part can stay close to the flat bottom by buoyancy. On the other hand, the energy needed for bubble injection is not small because those large ships have water depth of about 20m, against which bubbles have to be injected. Therefore it is necessary to reduce the amount of air and/or increase the drag reduction by studying the drag reduction mechanism and mininizing the amount of injected air. Recently some studies on the mechanism of skin friction reduction by microbubbles were carried out in Japan experimentally (Kato,1994, Guin,1996, Takahashi,1997, Kato,1998, Watanabe,1998). In this paper, some results of experimental efforts to find the dominant factor for skin friction reduction will be shown.

EXPERIMENTS

Test Facility

A closed circulating water tunnel specially designed for microbubbles was used in the experiments (Fig.1). Air is injected in the test section to generate bubbles, which are removed by buoyancy in a dump tank located downstream of the test section, thus making continuous tests possible.

The tunnel has a test section of 100mm × 15mm × 3000mm in size. The bubbles are generated by injecting air through

a porous plate made of sintered bronze with nominal pore radius of 10μm (Fig.2). The plate is located at 1038mm from the upstream end of the test section, where the flow is fully developed. This location is called Position 1, which is followed by Positions 2, 3, and 4, 500mm apart from each other, where various measurements are possible.

The amount of injected air is expressed by the average volume ratio $\overline{\alpha}_a$ defined as

$$\overline{\alpha}_a \equiv \frac{Q_a}{Q_a + Q_w} \tag{3}$$

where

Q_a : air flow rate through the porous plate

Q_w : water flow rate aross the full depth of the test

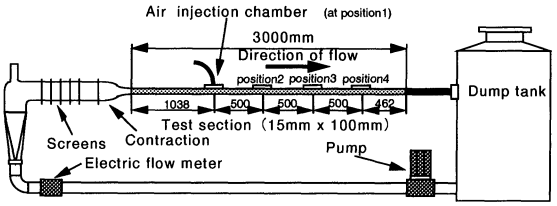

Figure 1 A circulating water tunnel for microbubble experiments

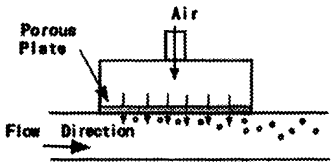

Figure 2 Bubble generation through a porous plate

Bubble Photographs

Photographs of the microbubbles were taken using a high-definition CCD camera. A light sheet generated by YAG laser was placed at 30mm from the center plane toward the camera (Fig.3). Fig.4 shows the photographs at $\overline{\alpha}_a$=0.053 at Positions 2 and 3. The flow is from right to left. The top end of each photo corresponds to the upper wall of the test section. The vertical length of the photo corresponds to 10mm. The bubbles are clustered near the top wall. The bubbles tended to diffuse toward downstream and at higher speeds. The size of the bubbles were mostly less than 1mm in diameter, being smaller at higher speeds.

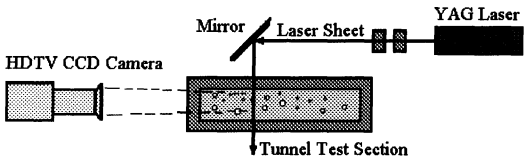

Figure 3 Camera and light source layout

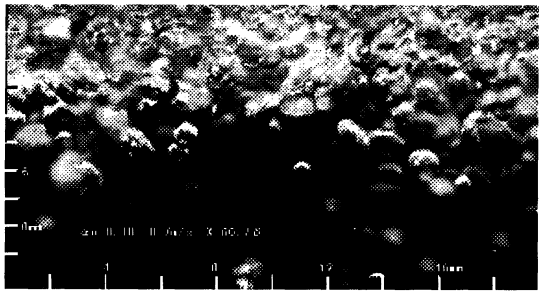

(a) U=7m/sec, Position 2

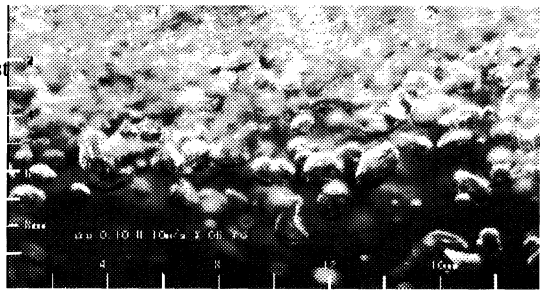

(b) U=7m/sec, Position 3

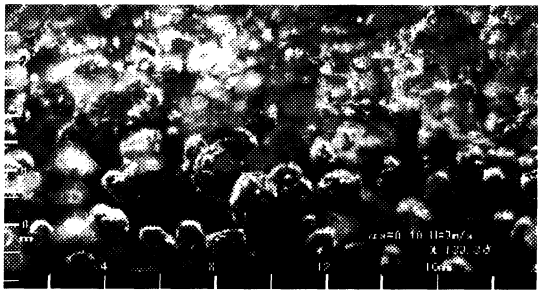

(c) U=10m/sec, Position 2

Figure 4 Photographs of microbubbles ($\overline{\alpha}_a$=0.053)

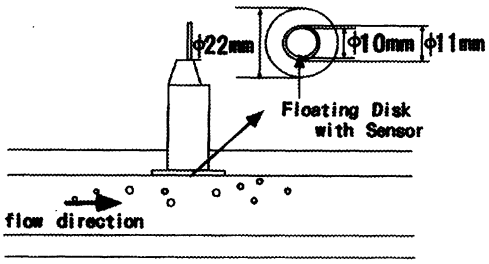

Figure 5 Skin friction sensor

Skin Friction Measurement

Skin friction sensors (Sankei Engineering co.,ltd.) of 2 grams full scale were used to measure skin friction directly (Kato, 1994) with or without bubbles (Fig.5). The sensor is a force gauge type with a sensing disk of 10mm diameter. The sensors were placed on the center plane of the test section.

Calibration

Static and dynamic calibrations of the skin friction sensors were made. In the static calibration the sensor was held horizontally so that gravity could be used in the calibration, and the weights of up to two grams were attached on the sensing disk using an adhesive tape. The result is shown in Fig.6. Two sensors were used in the calibration. The lines show the calibrations carried out by the manufacturer, and the symbols show those by the authors. They are in reasonable agreement.

In the dynamic calibration, the sensor was mounted flush on the upper wall surface of the test section, and the skin friction was measured in the non-bubble condition at various flow speeds. The result is shown in Fig. 7, in which the Blasius empirical formula (Schlichting, 1968) and the measured results based on pressure drops are also shown. The results by the skin friction sensors, obtained on three different dates, show some scatter. Although the results by the three methods show consistent deviation from each other, the overall tendency are similar, and it may be stated that this skin friction sensor can measure skin friction with reasonable accuracy.

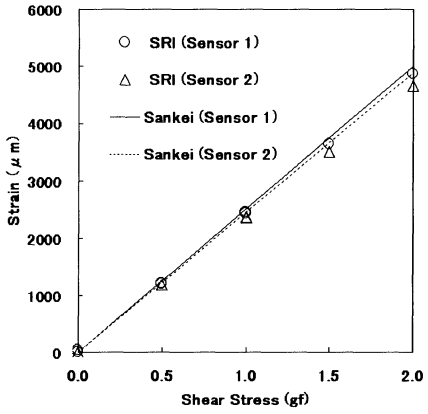

Figure 6 Static calibration of skin friction sensors

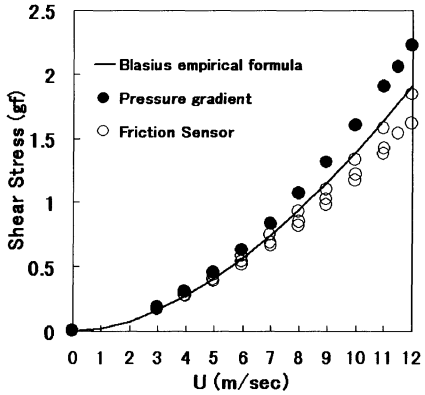

Figure 7 Dynamic calibration of skin friction sensors

Correction to C_{f_0}

In the following, the measured skin friction in the bubble condition is shown as the ratio to that in the non-bubble condition. But, in the bubble condition, i.e., when the air is injected in the test section, the flow speed increases due to the increase of the flow volume and therefore C_{f_0}, the skin friction in the non-bubble condition, needs to be corrected in the bubble condition. C_{f_0} was corrected as a function of Q_a using the following formulae.

$$C_{f_0}(Q_a) = C_{f_0}(0)\frac{\tau[U(Q_a)]}{\tau[U(0)]} \tag{4}$$

$$\tau(f) = 0.03325\rho\nu^{1/4}f^{7/4}r^{-1/4} \tag{5}$$

where

$C_{f_0}(Q_a)$: Corrected C_{f_0} at the air flow rate Q_a.
$U(Q_a)$: Average flow speed at Q_a
r : Hydraulic radius.

The eq.(5) corresponds to the empirical Blasius formula (Schlichting, 1968). The above two equations result in multiplying $C_{f_0}(0)$ by $[U(Q_a)/U(0)]^{\frac{7}{4}}$.

Measured Results

The skin friction was measured at three speeds in three streamwise locations. The results are shown in Fig. 8. Solid lines show an empirical formula obtained by Merkle (1990).

$$\frac{C_f}{C_{f_0}} = 0.8e^{-4\alpha_a} + 0.2 \tag{6}$$

At all the three speeds, the skin friction reduction increases as the amount of injected air increases. The maximum skin friction reduction was approximately 30%, while that of the experimental data eq.(6) is based on is 80%. It should be mentioned that those experimental data related to eq.(6) was obtained at only 50mm to 65mm downstream of the point of bubble injection, and the present data was obtained at 500mm to 1500mm downstream. At U=5m/sec the agreement of the present data with eq.(6) is good, but it becomes poorer at higher speeds, which might suggest that the correction using eq.(4) is reasonable but not good enough. In Fig.9, the streamwise change of skin friction reduction is plotted. The skin friction reduction is generally insensitive to streamwise locations. At U=10m/sec the skin friction reduction at Position 2 is greater than those at the other two locations.

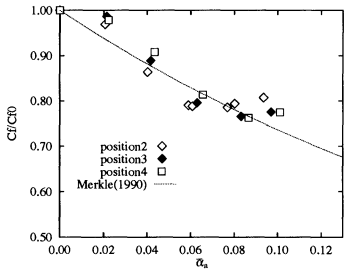

(a) $U = 5.0m/s$

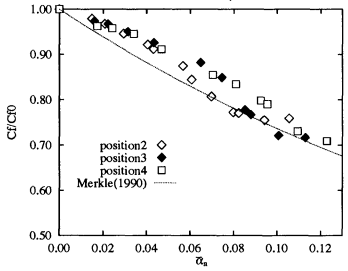

(b) $U = 7.0m/s$

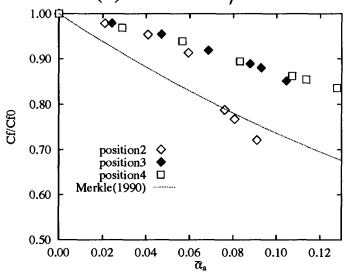

(c) $U = 10.0m/s$

Figure 8 Skin friction reduction by microbubbles (porous plate)

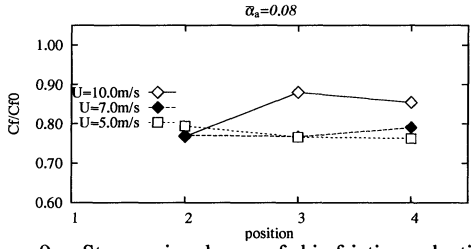

Figure 9 Streamwise change of skin friction reduction ($\bar{\alpha_a}$= 0.08, porous plate)

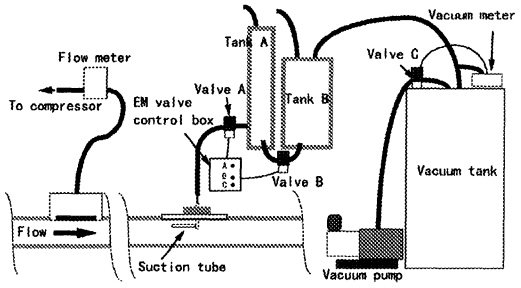

Figure 10 Suction tube to measure local void ratio

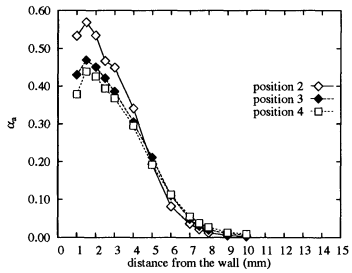

(a) $U = 5.0m/s$

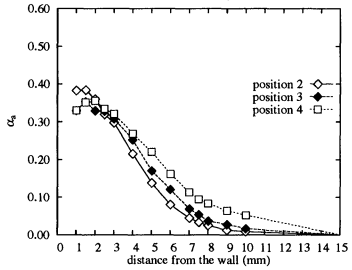

(b) $U = 7.0m/s$

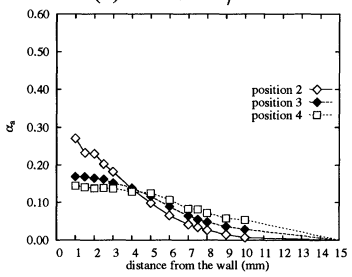

(c) $U = 10.0m/s$

Figure 11 Local void ratio α_a (uncorrected)

Local Void Ratio

The local void ratio α_a was measured using a suction tube system (Fig.10) similar to the one used by Guin (1996). A small tube with 1.2mm inner diameter and 1.6mm outer diameter was placed in the test section. The tube was connected to a vacuum pump for suction via two chambers to measure collected air and water volumes separately. The suction pressure was adjusted so that, in the non-bubble condition, the collected water volume was equal to that which passed through the suction area of the tube when the tube was not present in the flow. This means that the suction pressure was adjusted at each distance from the wall, and due to the pressure drop in the streamwise direction, at each streamwise location. The measurements were made at U=5, 7, and 10 m/sec. At U=5 and 7m/sec, the suction pressure was adjusted in the way described above, but at U=10m/sec the pressure was fixed at 0.105atm (80mmHg) because the low pressure in the downstream positions made the adjustment impossible.

The measured local void ratio α_a is shown in Fig. 11. The measured α_a was integrated in the test section by assuming constant distribution in the spanwise direction. The integrated air volume was 1.61 to 2.04 times that of the injected air

volume measured by the flow meter at U=5m/sec, 1.42 to 1.56 times at U=7m/sec, and 0.72 to 0.99 times at U=10m/sec. This excessive suction at two lower speeds was caused probably by the fact that the bubbly flow is more easily collected by the present system than water flow.

The measured local void ratio α_a shown in Fig. 11 was corrected so that the integrated air volume becomes equal to that of the injected air. The results are shown in Fig.12. At the low speed of U=5m/sec, the bubbles are clustered near the wall surface and hardly diffuse at downstream locations. They diffuse at higher speeds of U=7 and 10m/sec, and the degree of diffusion is greater as the speed becomes greater. At the highest speed of U=10m/sec, the bubbles diffuse significantly at downstream locations. When one compares the skin friction reduction plotted in Fig.9 with the local void ratio α_a closest to the wall, say $\alpha_{a_{\text{wall}}}$, plotted in Fig.12, they are seen to have strong correlation, i.e., the skin friction reduction becomes greater as $\alpha_{a_{\text{wall}}}$ becomes greater.

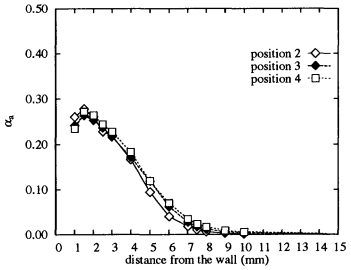

(a) $U = 5.0m/s$

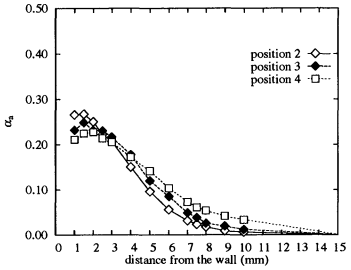

(b) $U = 7.0m/s$

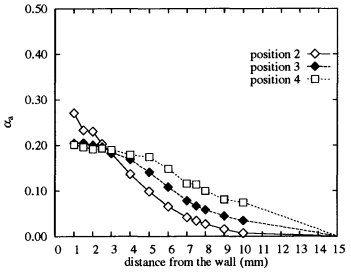

(c) $U = 10.0m/s$

Figure 12 Local void ratio α_a (corrected)

Array-of-Holes Plate

The porous plate used to generate bubbles has some problems. One is that only the nominal size of the holes is known. The other is the non-uniformity of the gerated bubbles, i.e., one observes that the size and number of the generated bubbles is not uniformly distributed on the porous plate. The third problem is that the pressure loss is not nominal.

In order to solve those problems, a new plate called array-of-holes plate was manufactured (Fig.13). On the plate, holes of 1mm diameter were made at the intervals of 5mm in the streamwise direction and 3mm in the spanwise direction. Using the array-of-holes plate, skin friction was again measured, and the results are shown in Fig.14. Comparing Fig.14 with Fig. 8, it is seen that skin friction reduction by the array-of-holes plate is comparable to that by the porous plate, except for the result at U=10m/sec and at Position 2, in which the skin friction reduction is much greater at higher void ratio using the porous plate, while that using the array-of-holes plate is comparable to others.

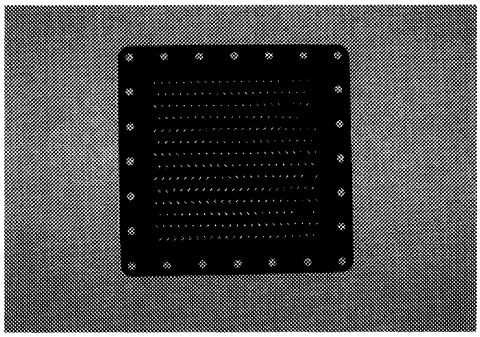

Figure 13 Array-of-holes plate

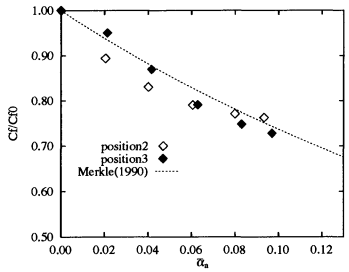

(a) $U = 5.0m/s$

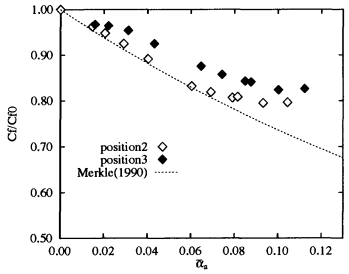

(b) $U = 7.0m/s$

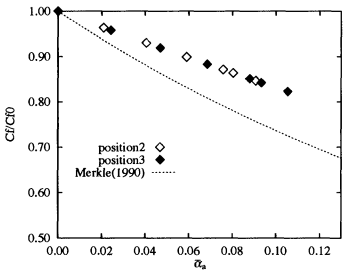

(c) $U = 10.0m/s$

Figure 14 Skin friction reduction by microbubbles (array-of-holes plate)

APPLICABILITY OF MICROBUBBLES TO SHIPS

In order to apply microbubbles to full scale ships, net drag reduction must be achieved. That is, the energy saved by skin friction reduction due to microbubbles must be larger than the energy spent to generate microbubbles against hydrostatic pressure at the bottom of a ship. Merkle carried out Here are some comments on the applicability of microbubbles to ships.
(1)The shallower the draft (water depth), the better. Recently designs of tankers of very shallow draft begin to be discussed. This kind of hulls have wider flat bottom area than usual, and therefore more suited to microbubbles.
(2)The gain due to microbubbles is dynamic, while the loss is static. Thus microbubbles are suited to fast ships.
(3)The scale effect of microbubbles must be clarified. In a towing tank Watanabe (1998) measured skin friction reduction by microbubbles on a flat plate 20m or 40m long and 0.6m wide, using skin friction sensors similar to those used in the present study (Fig.15). Bubbles were injected through a porous plate 250mm wide located at 1.2m from the front end. Merkle (1990) defined

$$Q_w = \delta U b \tag{7}$$

where δ is the boundary layer thickness and b is the width of the channel. Using this definition, the 1/7 power law for the velocity distribution, and eq.(6), the skin friction ratio C_f/C_{f_0} is estimated and shown in Table 2.

Table 2 Estimated C_f/C_{f_0} using eq.(6)
$Q_a = 0.005\text{m}^3/\text{sec}$ and U=7m/sec

distance from L.E. (m)	10	20	40
δ (m)	0.0998	0.174	0.303
$\overline{\alpha_a}$	0.0118	0.0068	0.0039
C_f/C_{f_0}	0.96	0.98	0.99

It is seen that the skin friction reduction shown in Fig.15 is much greater than that based on eq.(6). The reason for the discrepancy is not clear, since they measured no local properties except for the skin friction. Further studies in large scales are clearly needed.

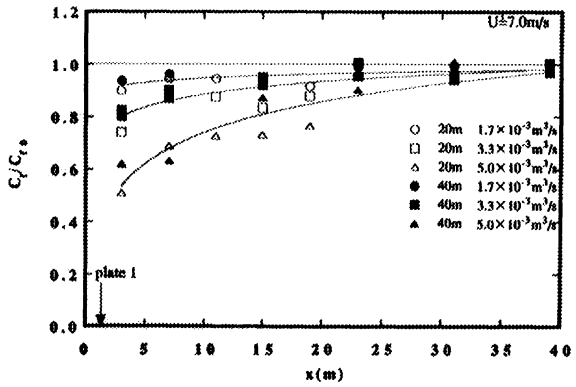

Figure 15 Skin friction reduction by microbubbles on 20m and 40m flat plates (Watanabe 1998)
U=7m/sec, $QQ_a = 1.7, 3.3,$ and$5.0 \times 10^{-3}\text{m}^3/\text{sec}$

CONCLUSIONS

Skin friction reduction by microbubbles was measured in a circulating water tunnel using skin friction sensors. The local void ratio was measured using a suction tube system. The results suggest that the local void ratio close to the wall is a dominant factor for skin friction reduction by microbubbles. Further studies are needed for clarifying the mechanism of skin friction reduction by microbubbles, especially in large scales, , in order to apply the method to full scale ships.

References

Guin, M.M. et al.,1996,"Reduction of Skin Friction by Microbubbles and its Relation with Near-Wall Bubble Concentration in a Channel", J. of Marine Science and Technology, Soc. Naval Arch. Japan, vol.1, No.5.

Kato, H. et al.,1994,"Frictional Drag Reduction by Injecting Bubbly Water into Turbulent Boundary Layer", Cavitation and Gas Liquid Flow in Fluid Machinery and Devices, FED-vol.190,ASME, pp185-194.

Kato, H. et al.,1998,"Effect of Microbubble Cluster on Turbulent Flow Structure", IUTAM Symposium on Mechanics of Passive and Active Flow Control, Gottingen. Merkle, C. and Deutsch, S.,1990,"Drag Reduction in Liquid Boundary Layers by Gas Injection", Progress in Astronautics and Aeronautics vol.123, AIAA.

Schlichting,H.,1968,"Boundary-Layer Theory", 6th edition, McGrawhill.

Takahashi,T. et al.,1997,"Streamwise Distribution of the Skin Friction Reduction by Microbubbles", J. of the Society of Naval Architects of Japan, vol.182.

Watanabe, O. et al.,1998,"Measurements of Drag Reduction by Microbubbles Using Very Long Ship Models", J. of Soc. Naval Architects, Japan, vol.183, pp.53-63.